Soil–Vegetation–Atmosphere Transfer Schemes and Large-Scale Hydrological Models (Proceedings of a symposium held during the Sixth IAHS Scientific Assembly at Maastricht, The Netherlands, July 2001). IAHS Publ. no. 270, 2001.

Estimating subsurface drainage from organic-covered hillslopes underlain by permafrost: toward a combined heat and mass flux model

W. L. QUINTON

Department of Geography, Simon Fraser University, Burnaby, British Columbia V5A 1S6, Canada

e-mail: bquinton@sfu.ca

D. M. GRAY

Division of Hydrology, University of Saskatchewan, Saskatoon, Saskatchewan S7N 0W0, Canada

Abstract Estimation of subsurface flow from organic-covered, permafrost terrain requires information on the elevation and thickness of the saturated layer because the soil permeability decreases with depth. Since heat conduction governs the thawing of seasonal frost, temperature index models might provide reasonable estimates of the rate of ground thawing. The depth of thaw derived from an estimate of ground heat flux is shown to be in close agreement with the measured depth to the frost table. Surface temperature is recommended as the index of heat flux rather than air temperature because it is directly influenced by the energy exchanges occurring at the ground/air interface and within the active layer and its value can be estimated from remotely-sensed thermal infrared data. It is shown that the coefficient C of the relationship between friction factor, f and Reynolds Number, N_R, (i.e. $f = C/N_R$) increases linearly with the depth to the middle of the saturated zone, d. Since $C = 2D^2/K$, where D is the geometric mean pore diameter of the material encountered by the saturated layer, and K is the soil permeability, the relationship between C and d allows an approximation of the variation in permeability with depth.

Key words subsurface drainage; permafrost; soil thaw; coupled heat and mass flow

INTRODUCTION

Estimation of subsurface flow from organic-covered hillslopes underlain by permafrost requires that the elevation of the saturated layer be known, since the saturated hydraulic conductivity of the organic material decreases exponentially with depth (Quinton *et al.*, 2000). An algorithm of coupled heat and mass flow combined with a lateral routing routine would enable estimates of subsurface runoff from these hillslopes during soil thawing. Colbeck (1974) presented a procedure describing laminar flow through a slush layer at the base of a melting snowpack that would serve as a framework for modelling subsurface flow through organic soils (or other porous media). If used for this purpose his solutions would require modification because: (a) they assume an impermeable ground surface, whereas average infiltration rates of 188.4 m day^{-1} (Dingman, 1973) and 197.3 m day^{-1} (Quinton *et al.*, 2000) have been reported for tundra environments, and (b) they do not account for changes in hydraulic

conductivity with depth, whereas in arctic tundra a two to three order of magnitude decrease in soil permeability in the depth increment 0–30 cm has been measured (Quinton & Marsh, 1999). Correct delineation of subsurface lateral flow in arctic tundra will require reliable methods for estimating (a) the hydraulic conductivity as a function of the depth of the saturated layer, and (b) the elevation of the saturated layer.

Quinton *et al.* (2000) related the physical properties of organic soils in the arctic tundra to their transmission properties. As an extension of that study, the objectives of this paper are to: (a) present preliminary results of ongoing studies relating soil thermo-physical properties to the seasonal thaw of the organic soils, and (b) recommend a physically-based approach of estimating the flow of mass and energy through these soils.

STUDY SITES

Most of the field research was conducted in Canada at Siksik Creek (68°44′N, 133°28′W) at the northern fringe of the forest–tundra transition (Bliss & Matveyeva, 1992), 55 km north-northeast of Inuvik, Canada, in the continuous permafrost zone (Heginbottom & Radburn, 1992). Selected measurements were conducted at two other organic-covered, permafrost basins: Granger Creek (60°31′N, 135°07′W), in alpine tundra 15 km south of Whitehorse, Yukon Territory, and Scotty Creek (61°18′N, 121°18′W), in the wetland-dominated high boreal region of the lower Liard River valley, 55 km south of Fort Simpson, Northwest Territories. All three sites have a continuous organic cover, with the thickest at Scotty Creek (~0.4–0.6 m), followed by Siksik (~0.2–0.5 m), and Granger (~0.2–0.35 m). By late summer, the average frost table depth is ~0.6 m at Scotty, 0.4 m at Granger, and 0.3 m at Siksik.

METHODOLOGY

Tracer tests were conducted at Siksik Creek in 1993 and 1994, at Scotty Creek in 1999 and 2000, and at Granger Creek in 2000. Quinton & Marsh (1999) provide a detailed description of the tracer experiments. The average pore velocity v, was computed as:

$$v = (L_X/t_c)\cdot T_x \quad (1)$$

where L_X is the straight-line distance between the tracer application line and sensing electrode, and t_c is the length of time between the application of the tracer and the time when the centre of mass of the tracer plume reached the sensing location. T_x is the average tortuosity of flow resulting from the presence of mineral earth hummocks. At Siksik Creek, T_x ranges between 1.1 and 1.5 (Quinton & Marsh, 1999) while at the Granger and Scotty sites, where no hummocks occurred, $T_x = 1$. The friction factor f, was computed from:

$$f = [2g(S/T_x)D]/v^2 \quad (2)$$

where g is gravitational acceleration, S is the energy slope, and D is the geometric mean pore diameter of the soil in the saturated zone.

Soil moisture and temperature were monitored at Scotty Creek in 1993. The volumetric liquid water content was measured using time domain reflectometry, at 5,

Table 1 Volumetric composition of soils, and thermal properties used for computations.

Layer	Soil type	Depth (m)	Porosity ϕ	Density ρ (kg m^{-3})	Specific heat* c (J kg^{-1} K^{-1})	Heat capacity† Cv (J m^{-3} K^{-1})	Thermal cond. λ (W m^{-1} K^{-1})	Hydraulic cond. k (m day^{-1})
1	organic	0.05–0.15	0.96	41.1	1920	78 912	0.21	450
2	organic	0.15–0.25	0.90	75.2	1920	144 384	0.21	154
3	organic	0.25–0.35	0.87	91.4	1920	175 392	0.21	13
4	mineral	0.35–0.45	0.43	1300	890	1 157 000	2.5	5
Air	–	–	–	1.2	1010	1 212	0.025	–
Ice	–	–	–	920	2120	1 950 400	2.24	–
Water	–	–	–	1000	4185	4 185 000	0.57	–

* Values obtained from Miller (1981) and Oke (1987).
† Heat capacity of the soil phase.

15, 22 and 38 cm below the ground surface. In the same profile, soil temperatures were measured with thermistors at 8, 20, 30 and 45 cm depth. Based on the vertical spacing of the moisture and temperature sensors, the active layer was conceptualized as containing three organic layers (0.05–0.15 m, 0.15–0.25 m and 0.25–0.35 m), overlying a mineral layer (0.35–0.45 m) (Table 1). In addition, measurements of the depth of the frost table below the ground surface were made weekly along a transect at fixed distances from the edge of a stream using a graduated steel rod. The depth to the water table was recorded with a Stevens Type-F recorder housed on a well.

The volumetric heat capacity of the mineral or organic material of each soil layer was calculated from the product of the bulk density and the specific heat, with values of the latter obtained from the literature (Table 1). The composite volumetric heat capacity of each soil layer was computed from the constituent volumetric heat capacities using equations (3), (4), or (5). Equation (3) was used if the soil layer was unsaturated and unfrozen, equation (4) if the layer was saturated and frozen, and equation (5) if it was saturated and unfrozen:

$$Cv_{WSA} = Cv_W\,\theta + C_S\,(1 - \phi) + Cv_A\,(\phi - \theta) \tag{3}$$

$$Cv_{IWS} = Cv_I\,(\phi - 2) + Cv_W\,\theta + Cv_S\,(1 - \phi) \tag{4}$$

$$Cv_{WS} = Cv_W\,\theta + Cv_S\,(1 - \phi) \tag{5}$$

where Cv is the volumetric heat capacity, θ is the volumetric soil moisture, ϕ is the porosity, and the subscripts W, S, A and I refer to water, soil, air and ice constituents, respectively. An unsaturated and frozen condition did not occur at the measurement depths, and therefore the value of Cv for this condition was not computed. The thermal conductivity, λ was computed using the equations provided by Farouki (1981). For the saturated, unfrozen (λ_{WS}) condition, λ was computed from:

$$\lambda_{WS} = \lambda_w a^2 + \lambda_s(1 - a)^2 + \{\lambda_s\lambda_w(2a - 2a^2)/[\lambda_s(a) + \lambda_w\,(1 - a)]\} \tag{6}$$

For the saturated, frozen case, λ_W in equation (6) was replaced with the thermal conductivity of ice, λ_I. For the unfrozen, unsaturated condition (λ_{WSA}), λ was computed from:

$$\lambda_{WSA} = (x_w\lambda_w + F_a x_a\lambda_a + F_s x_s\lambda_s)/(x_w + F_a x_a + F_s x_s) \tag{7}$$

where a is calculated from the soil porosity using formulae provided by Farouki (1981), x is the volume fraction in a unit soil volume. F_s is the ratio between the space average of the temperature gradient in the solid relative to the water phase, and F_a is the corresponding ratio for the thermal gradient in the air and water phases. Both F_s and F_a were computed from formulae presented by Farouki (1981).

The Trail Valley Creek meteorological station (Environment Canada) located within the Siksik Creek catchment provided additional data. At this site, ground heat flux was measured with a flux plate inserted at 4 cm depth, air temperature was measured at 1.2 m, and surface temperature was measured with an infrared sensor. However, the station was operable for only a relatively short period in 1993, and as a result, the data were of limited use for this study.

Soil cores containing the entire thickness of the peat layer were extracted close to the location of the soil moisture–temperature profile at Siksik Creek. Sub-samples were taken from the soil cores at depths corresponding to the moisture and temperature measurements, in order to measure the bulk density and total porosity. Soil thin sections (~100 μm thick) were prepared and photographed for measurement of pore diameters using image analysis software (Quinton & Marsh, 1999).

RESULTS AND DISCUSSION

Seasonal variation in soil thermal properties

Over the study period, the composition of the upper two soil layers, adjusted from an ice–water–soil mixture to one of water and soil only, and finally to an unsaturated mixture of water–soil–air. The lower two soil layers experienced only the first and second of these compositional stages, as they were almost always saturated. As a result, layers 1 and 2 experienced three distinct levels of volumetric heat capacity (Fig. 1(a)) and thermal conductivity (Fig. 1(b)), while layers 3 and 4 experienced only two levels.

The downward development of the saturated zone through the soil profile during soil thawing increases the volumetric heat capacity (Fig. 1(a)) of the lower soil layers due to the increase in specific heat that accompanies the phase change of ice to water (see Table 1). Conversely, the average thermal conductivity in all soil layers (Fig. 1(b)) decreases as the thawed layer thickened due to the replacement of ice, a highly conductive medium, by water. Figure 1(b) shows the decrease in thermal conductivity is greatest in layer 1 where the porosity is highest (~0.96), and least in the mineral sediment, where the porosity is only ~0.43 (Table 1).

Ground heat flux

Assuming heat flow into the ground occurs primarily by conduction and the amount of energy supplied by convection can be safely ignored (Woo & Xia, 1994), the ground heat flux, Q_G can be computed from (Fuchs, 1986):

$$Q_G = Q_A + Q_P + Q_M \tag{8}$$

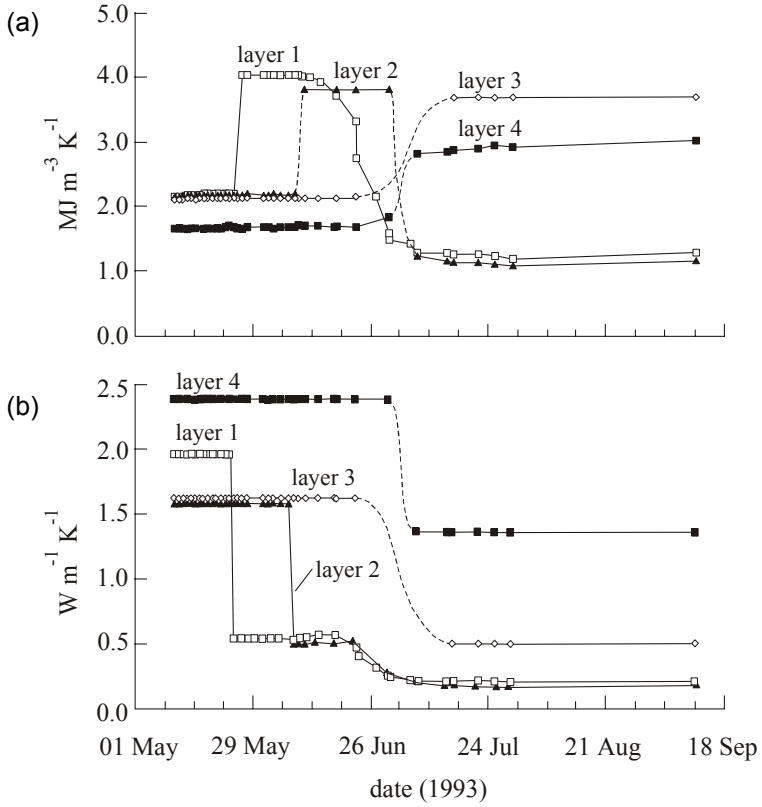

Fig. 1 Variations in (a) the volumetric heat capacity, and (b) thermal conductivity computed for each soil layer at Siksik Creek.

where Q_A is the energy used to warm the active layer, Q_P is the energy used to warm the permafrost, and Q_M is the energy used to melt ice in the active layer. Daily totals of each component summed over the study period show that Q_M (48%) and Q_P (45%) consume most energy entering the ground surface and that Q_A is a relatively minor component (7%).

A cumulative plot of Q_A for each soil layer provides a reasonable estimate of the heat stored in each layer, as indicated by the close agreement of Fig. 2(a) with the measured temperature profile, Fig. 2(b). The vertical temperature distribution in the soil is strongly affected by the elevation of the thawed saturated zone as indicated by the water table position in Fig. 2(b). As a soil layer drains, becoming unsaturated, its heat capacity decreases, which causes an increase in temperature (Fig. 2(b)). The strong temperature gradients that develop close to the ground surface (Fig. 2(b)), result from the fact that over half of the total energy used to warm the active layer, is consumed in layer 1 (Fig. 2(a)).

Prediction of soil thaw and mass transfer

Assuming heat flow by conduction is the primary process that governs soil thawing, it is reasonable to expect that a temperature-based model would provide estimates of the ground heat flux. Previous energy balance studies in arctic tundra (Abbey *et al.*, 1973) suggested that a simple degree-day temperature model gave a reasonable approx-

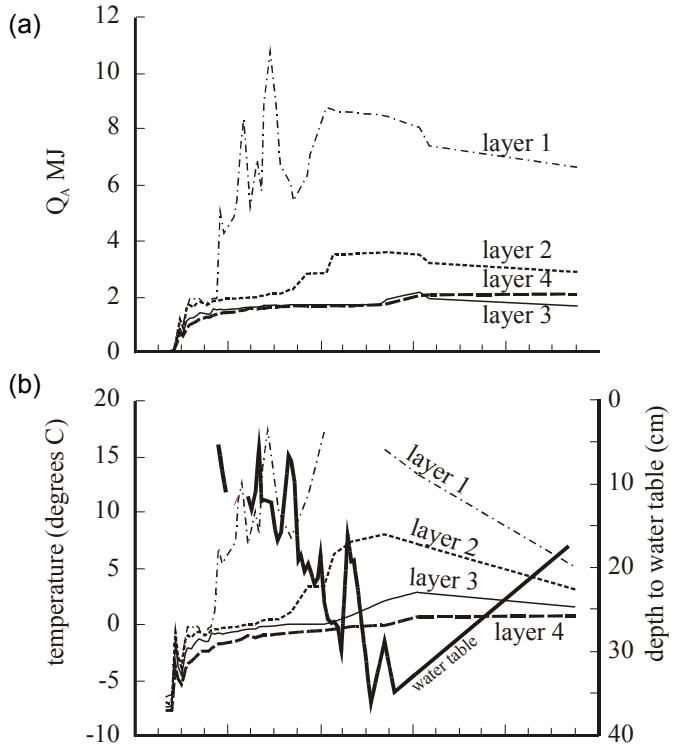

Fig. 2 (a) Cumulative values of Q_A computed for each soil layer, and (b) variations in temperature and water table elevation at Siksik Creek.

imation of soil thawing. A plot of the cumulative mean daily air temperature (ΣTa) from the first snow-free day, computed from measurements at the meteorological tower, and the cumulative daily Q_M (Fig. 3(a)), suggests the relationship:

$$\Sigma Q_M = 0.0061\Sigma Ta + 0.00000009(\Sigma Ta)^2 - 8.4593 \qquad (r^2 = 0.99) \tag{9}$$

Despite the strong correlation between cumulative ground heat flux and air temperature shown in equation (9), such regressions have only limited value as a predictive tool because air temperature is not independent of factors other than the energy exchanges occurring at and below the tundra surface. The weakness restricts the transposability of an empirical association for estimating the ground heat flux at a site where soil thermophysical properties may differ appreciably from those where the regressions were derived. A preferred approach uses surface temperature as an index rather than air temperature since surface temperature is directly influenced by the surface energy exchanges (Fig. 3(b)). This approach also offers the prospect of using remotely sensed, thermal infrared data as a method of obtaining the input variable for the model.

Quinton *et al.* (2000) used expressions of head loss from Weisbach (Rouse & Ince, 1957) and Darcy to derive an expression for the friction factor f, and showed that if the geometric mean pore diameter D and the value of the coefficient C in the relationship $C = f/N_R$ (N_R = Reynolds number) are known, then the permeability K can be estimated from $K = 2D^2/C$, from which the hydraulic conductivity (k) is obtained (i.e. $k = K\rho g/\mu$, where ρ and μ are the density and dynamic viscosity of water, and g is acceleration due to gravity). Because the rate of water transmission through the peat decreases as

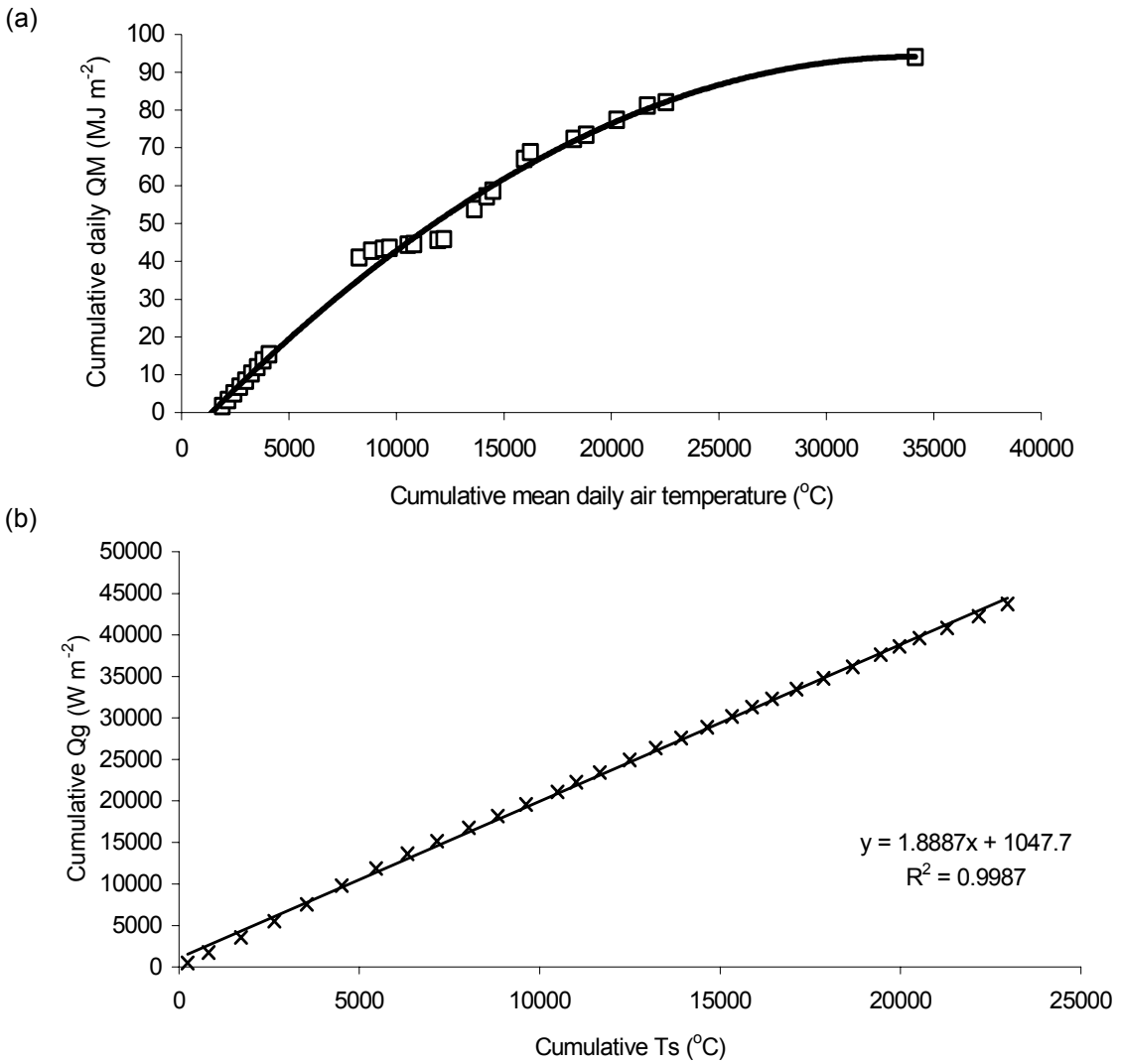

Fig. 3 Relationship between (a) the cumulative daily air temperature and the cumulative daily energy used to melt ice, Q_M in the active layer, i.e. lower the frost table, and (b) the daily cumulative ground heat flux and daily cumulative surface temperature, at Siksik Creek, 1993.

the depth to the middle of the saturated zone d increases (Quinton *et al.*, 2000), obtaining a reasonable estimate of C, requires that the value of d be known. As a first approximation, d can be approximated from equation (9). It is also necessary that a C–d relationship be defined. Since $C = 2D^2/K$, a C–d relationship would allow an approximation of the variation in permeability with depth from estimates of the variation in mean pore geometry with depth, obtained from laboratory analysis of soil samples. Based on further analysis of the data presented by Quinton *et al.* (2000), and on the additional data from the Scotty and Granger sites, it was found that there is a strong tendency for C to increase linearly with depth (Fig. 4):

$$C = 91586d - 8321.8 \qquad (r^2 = 0.90) \tag{10}$$

An expression in the form of equation (10) forms the basis of the hydraulics of a flow model.

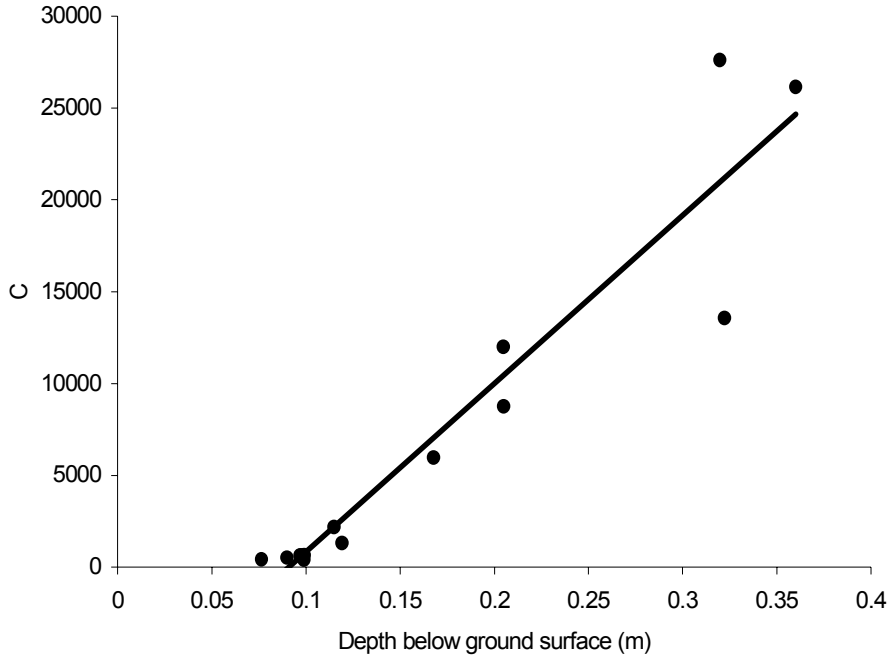

Fig. 4 A plot of C and depth of the middle of the saturated layer below the ground surface. The plot is based on data collected at Siksik Creek (Quinton *et al.*, 2000) and at Granger and Scotty Creeks.

CONCLUSIONS

Field studies conducted in organic-covered, permafrost terrain, examined the thermal regime of the active layer and subsurface runoff during snow ablation and ground thawing. The results of these studies suggest a physically-based approach for estimating the rate of drainage through the saturated layer from physical, hydraulic and thermal properties of the active layer. The relationship between C (i.e. where $C = 2D^2/K$) and the depth to the midpoint of the thawed saturated layer, d based on observations from three organic terrain types, allows an approximation of the variation in permeability with depth from estimates of the variation in mean pore geometry with depth and saturated layer position. The strong correlation between cumulative degree-day air temperature and cumulative Q_M, suggests that temperature index models can provide reasonable estimates of the frost table elevation. The frost table depth can be used as a surrogate for, or a means of estimating the saturated layer elevation, needed to estimate the value of C from the C–d relationship. Future studies should use surface temperature rather than air temperature in the temperature index association, since surface temperature is directly affected by the energy exchanges occurring at the soil surface and the thermal properties of the active layer. This would enhance the transposability of empirical expressions to other organic terrain types.

REFERENCES

Abbey, F. L., Gray, D. M., Male, D. H. & Erickson, D. E. L. (1978) Index models for predicting heat flux to permafrost during thawing conditions. In: *Proc. Third International Conference on Permafrost*, vol. 1, 3–9. National Research Council of Canada, Ottawa, Canada.

Bliss, L. C. & Matveyeva, N. V. (1992) Circumpolar arctic vegetation. In: *Arctic Ecosystems in a Changing Climate: An Ecological Perspective* (ed. by F. S. Chapin III, R. L. Jefferies, J. F. Reynolds, G. R. Shaver & J. Svoboda), 59–89. Academic Press, San Diego, USA.

Colbeck, S. C. (1974) Water flow through snow overlying an impermeable boundary. *Wat. Resour. Res.* **10**, 119–123.

Dingman, S. L. (1973) Effects of permafrost on stream flow characteristics in the discontinuous permafrost zone of central Alaska. In: *Permafrost: the North American Contribution to the Second Int. Conf.* (Yakutsk, USSR), 447–453. Washington, National Academy of Sciences, Washington, USA.

Farouki, O. T. (1981) The thermal properties of soils in cold regions. *Cold Regions Sci. Technol.* **5**, 61–65.

Fuchs, M. (1986) Heat flux. In: *Methods of Soil Analysis, Part 1, Physical and Mineralogical Methods* (second edn) (ed. by A. Klute), 957–968. Soil Sci. Soc. Am., Madison, Wisconsin, USA.

Heginbottom, J. A. & Radburn, L. K. (1992) *Permafrost and Ground Ice Conditions of Northwestern Canada*. Geol. Survey of Canada, Map 1691A, scale 1:1 000 000. Geol. Survey of Canada, Ottawa, Canada.

Quinton, W. L. & Marsh, P. (1999) Image analysis and water tracing methods for examining runoff pathways, soil properties and residence times in the continuous permafrost zone. In: *Integrated Methods in Catchment Hydrology* (ed. by C. Leibundgut, J. McDonnell & G. Schultz) (Proc. Symp. HS4, IUGG 99, Birmingham, July 1999), 257–264. IAHS Publ. no. 258.

Quinton, W. L., Gray D. M. & Marsh, P. (2000) Subsurface drainage from hummock-covered hillslopes in the Arctic tundra. *J. Hydrol*. **237**(1–2), 113–125.

Rouse, H. & Ince, S. (1957) *History of Hydraulics*. Edwards Bros. Inc., Ann Arbor, Michigan, USA.

Woo, M. & Xia, Z. (1994) Effects of hydrology on the thermal conditions of the active layer: hydrological processes and runoff at the Arctic treeline in Northern Canada. In: *Proc. Tenth Int. Northern Research Basins Symp. and Workshop* (Svalbard, Norway) (ed. by K. Sand & A. Killingtveit), 429–448.